

Reduction of magnetic noise limits of orthogonal fluxgate sensor

Michal Dressler^{1, a)}, Michal Janosek¹ and Mattia Butta¹

1) Department of Measurement - Faculty of Electrical Engineering, Czech Technical University in Prague, Technická 2, 16627 Prague, Czech Republic

a) Corresponding author: dressmic@fel.cvut.cz

Abstract. We have further lowered the white noise of an orthogonal fluxgate to about 0.3 pT/√Hz @ 8 Hz. So far, this is the lowest noise reported for a fluxgate magnetometer. The noise reduction was achieved by introducing a JFET input stage, embedded directly to the sensor head, allowing for high common-mode rejection and negligible loading of the resonant circuit. The origin of the noise was investigated by correlation measurements and we concluded that, at least in the white noise region, we observe the magnetic noise of the sensor, with about 0.1 pT/√Hz white noise contribution by the electronics. We were finally able to obtain sensor noise floor below 1 pT/√Hz @ 1 Hz also in a feedback-compensated closed-loop. Closed-loop operation allows for higher magnetometer stability and operation in Earth's magnetic field without deteriorating its noise performance.

INTRODUCTION

The orthogonal fluxgate sensors based on magnetic microwires, when operated in fundamental mode with DC bias^{1,2}, show perspective for sub pT-level vectorial magnetic sensors at room-temperature. However, decreasing the magnetic noise values close or below 1 pT puts strong demands not only on manufacturing the sensor^{3,4}, but also on the performance of its conditioning electronics. So far, the lowest noise was achieved using fluxgates with Π -shaped magnetic core made from amorphous wires^{5,6}. Specifically, we used a sensor head with four Co-rich AC20 UnitikaTM wires with 120 μm diameter - see Fig. 1a. The wires have been annealed for 6 minutes by Joule heating with a 2 second polarity switch⁷. The process of annealing is necessary to increase the circular anisotropy, which leads to lower energy of the minor loops for a given excitation current. The effect of annealing is also visible in the MOKE images we have obtained with a Kerr Microscope and KerrLab software (evico-magnetics, Dresden, Germany) - see Fig 1b. The as-cast (C) and annealed (A) wires were fed by the same current with two different values - 0.2 and 2 mA. While the as cast wire is still composed of multiple bamboo-like domains with the 2-mA excitation, the annealed wire already exhibits a single, large domain which flips polarity between those two levels.

The optimization of the wire core however pushed the design of our magnetometer to its limits. Recently, we were able to achieve about 0.8 pT/√Hz noise density at 1 Hz and 0.8 pT/√Hz noise floor with an open-loop operated magnetometer⁵. The electronic unit consisted of a multichannel DDS, a stable current source for magnetic wire excitation⁸ and two independent pickup preamplifiers and demodulators - see Fig. 1c. The limiting factor in terms of noise was found as the pickup coil preamplifier and the rejection of excitation feed-through and other EMI signals. Also, we experienced an increase of the noise to 1.5 pT/√Hz when operated in the feedback loop.

If we want to achieve further noise reduction, we should then reduce the noise of the input stage (amplifier), which is a crucial component of the magnetometer. In this paper we address this noise and we propose a new circuit which reduces the noise by removing the loading of the pick-up coil.

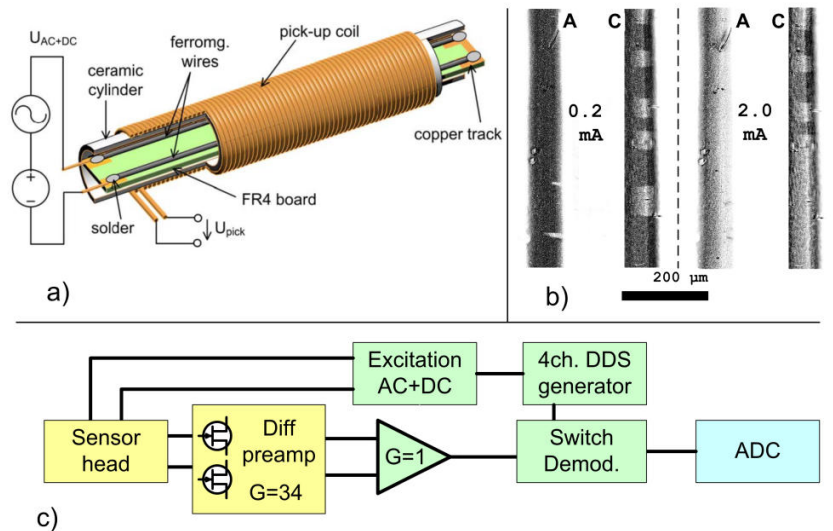


Fig. 1. a) The orthogonal fluxgate sensor head structure⁵. Reproduced with permission from IEEE Trans. Inst. Meas 69, 2552 (2020). Copyright 2020 IEEE. b) Superimposed topology and MOKE image of microwire magnetic domains on as-cast and Joule annealed wire. c) Simplified magnetometer circuit block diagram.

IDENTIFYING THE LIMITATIONS

We have investigated the limitations of our initial design^{5,6}. Here, a simple difference amplifier with LT6234 op-amp was used – the equation for its equivalent voltage noise e_{out} is following:

$$e_{out} = \sqrt{2(i_n R_2)^2 + (e_n(NG + 1))^2 + 8kT(R_2 + R_1 \cdot NG^2)}, \quad (1)$$

(2)

$$NG = \frac{2 \cdot R_2}{2 \cdot R_1 + Z_c}$$

The gain of 30 was set with two feedback resistors $R_1 = 1 \text{ k}\Omega$ and $R_2 = 30 \text{ k}\Omega$, the opamp input voltage noise density was $e_n = 2 \text{ nV}/\sqrt{\text{Hz}}$ and its current noise was $i_n = 0.8 \text{ pA}/\sqrt{\text{Hz}}$. In addition, we need to take into the account the effect of coil impedance Z_c at resonance on the noise-gain NG of the amplifier in Eq. 2. Taking into account all noise contributions of Eq. 1, the resulting noise e_{out} is equal to $240 \text{ nV}/\sqrt{\text{Hz}}$ or $8 \text{ nV}/\sqrt{\text{Hz}}$ when referred to input.

Moreover, the low input resistance of the differential amplifier ($\sim 2 \text{ k}\Omega$) dampens the pickup resonant circuit (about $5 \text{ k}\Omega$ equivalent LC tank impedance Z_c at 40 kHz), resulting in lowering magnetometer sensitivity approx. to $1/4$. The noise contribution of a switching-type demodulator adds another $12 \text{ nV}/\sqrt{\text{Hz}}$ RTI (measured with its input shorted). All these noise sources combined together create a hardware noise limit of $14.4 \text{ nV}/\sqrt{\text{Hz}}$. If we know the sensor sensitivity (before amplification) - about 22 kV/T - we end up with approx. $0.65 \text{ pT}/\sqrt{\text{Hz}}$ white noise, which was the noise limit presented⁵. However, having the noise of the electronics at the same level of the total noise of the magnetometer does not allow to reveal the actual noise of the sensor, and this is the ultimate limit to reduce the total noise.

CIRCUITRY IMPROVEMENTS

In order to reduce the capacitively-coupled excitation feed-through, at the cost of lower sensitivity, we have decreased the pick-up coil number of turns from 2000 (4-layers) to approximately 1000 (2-layers). This also allowed to decrease the pickup coil impedance from $5 \text{ k}\Omega$ to $2 \text{ k}\Omega$. We could also use higher gain in the input stage to minimize noise contribution of following stages (demodulator and acquisition circuits).

J-FET Input Stage

In order to avoid loading of the resonant circuit and thus maximize the sensitivity, we have added a J-FET differential amplifier stage before the difference amplifier (Fig. 2). This stage consists of a low-noise LSK389 matched transistor pair with $1.9 \text{ nV}/\sqrt{\text{Hz}}$ white input voltage noise density and negligible input current noise. The gain of the J-FET pre-amplifier stage was set to 34 and it is followed by a differential to single-ended receiver with gain 1. The JFET preamplifier is built on a PCB together with the sensor, in order to obtain high common-mode-rejection ratio and avoid long cabling with high impedance signals (Fig. 2.).

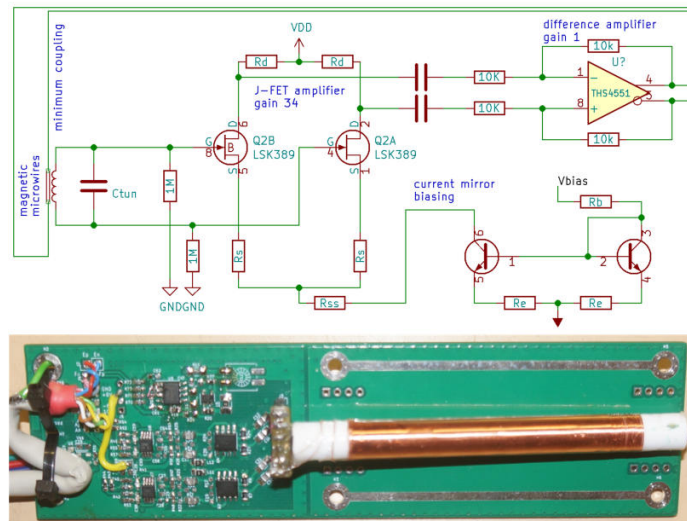


Fig. 2. Simplified schematics of pickup coil input stage (top) and a photo of finished board including two independent input channels (bottom) connected directly to sensor head.

Since the J-FET amplifier does not load the LC tank, we observe a significant sensitivity increase at the resonance frequency – see Fig. 3a. The magnetometer sensitivity with the same excitation parameters (48 mA AC at 44 kHz) is five times higher than with the simple diff op-amp - 30-35 kV/T. Higher sensitivity leads to an expected decrease of the measurable sensor noise floor, which dropped from $0.6 \text{ pT}/\sqrt{\text{Hz}}$ to $0.15 \text{ pT}/\sqrt{\text{Hz}}$ - Fig. 3b. More importantly, we achieved a noise reduction also in the $1/f$ region; the noise density at 1 Hz measured on the sensor dropped from $1 \text{ pT}/\sqrt{\text{Hz}}$ to $0.7 \text{ pT}/\sqrt{\text{Hz}}$. We can also see the effect of increased CMRR and noise suppression by having the preamplifier stage close to the sensor - the spikes seen with the previous design completely disappeared.

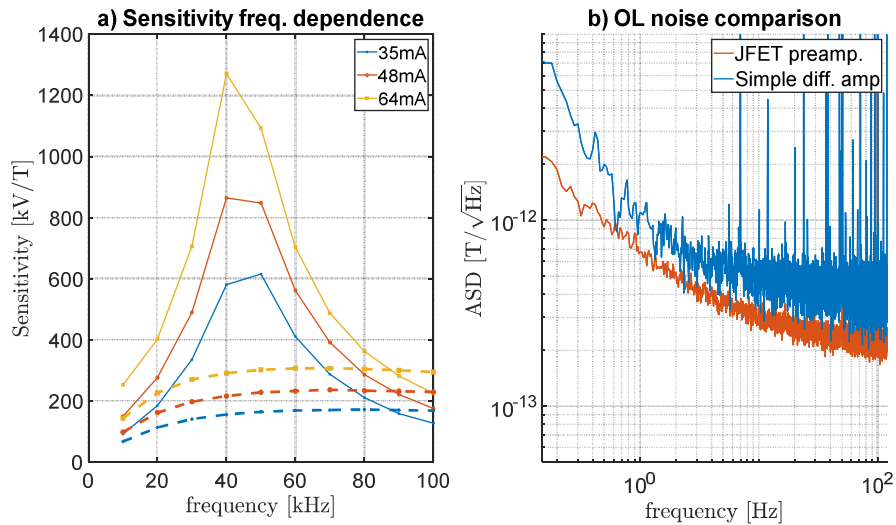


Fig. 3. a) Comparison of magnetometer sensitivity frequency dependence using simple diff-amp (dashed) and an improved JFET amplifier stage (solid). b) Magnetic noise spectrum density measured in a 6-layer Mu-metal shield.

INVESTIGATING THE NOISE ORIGIN

To further distinguish the noise of the electronics from the noise of the sensor, we have utilized both magnetometer input channels and two sensors for correlation measurements. We have measured the cross-spectrum density using only one sensor connected to two independent inputs and acquisition channels in parallel. Later, we measured with two individual sensor heads, placed several centimeters apart, pointing to the same direction and again connected to independent inputs, but sharing common excitation current. The measurements shown in this chapter were done in a 6-layer Mu-metal shield, and the sensors were operated in open loop mode to eliminate the possibility of feedback compensation cross-talk.

Assuming no correlation in the amplifier stages of the input channels, the possible remaining origins of correlation are:

- Common excitation current noise⁸
- Demodulators reference jitter correlation (reference is driven from single four-channel DDS IC)
- Shielding remanence noise (which is however in fT range⁹)
- Magnetic field noise (residual noise in the shielding due to finite shielding factor)
- Magnetic coupling of closely placed sensors¹⁰
- Noisy feed-through signal (by capacitive and transformer coupling from excitation)

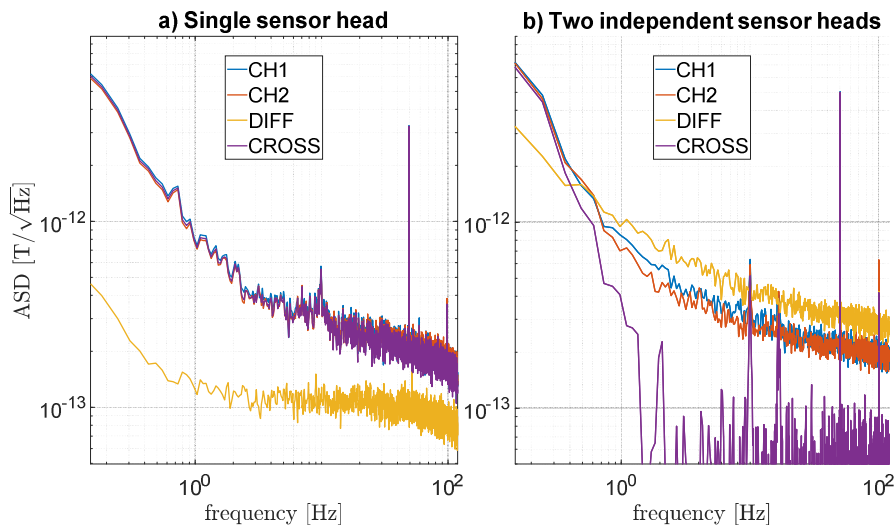


Fig. 4. Noise density of simultaneously measured independent input channels CH1 and CH2. DIFF is CH1-CH2 difference and CROSS is their cross-spectrum density. a) Correlation measurement of single sensor head connected to both input channels. b) Correlation measurement of independent sensor heads with common excitation.

From the theory, the DIFF (noise density of time-domain difference of CH1 and CH2) values in Fig. 4. should either increase for uncorrelated noise signals CH1 and CH2 by a factor of $\sqrt{2}$, or for correlated signals it should drop down to the noise floor limit of the acquisition. Similarly, the CROSS (cross-spectrum density) value should drop for uncorrelated noise sources and should not change for correlated signals.

From the cross-spectrum measurement on a single sensor connected to two independent channels (Fig. 4a), we conclude that the observed noise is fully correlated (no change of CROSS density and DIFF density drops to 150 fT/ $\sqrt{\text{Hz}}$ floor).

The correlation measurement of two independent sensor heads placed side by side about 5 cm apart – see Fig. 4b – gives evidence that the measured noise limit is truly a property of the given sensors, as the noise at higher frequencies is not correlated (DIFF increases, CROSS drops). On the opposite, the noise in 1/f section below 1 Hz seems to be correlated, most likely because it is actually the Earth’s magnetic field noise not sufficiently attenuated by the Mu-metal magnetic shielding. To use the two sensor heads as a gradiometer, also a proper astatization (sensors axes numerical alignment) would be necessary.

CLOSING THE LOOP

Feedback loop operation of a magnetometer is advantageous not only for increasing the measurement range but also for decreasing the effects of gain instability with time and temperature. In order to close the feedback loop, we added a V/I converter with ADA4004-1 to our sensor head electronic; the V/I converter is driven by a differential receiver-amplifier. In this manner, we could design the integrator (feedback I-controller) circuit as a part of the remote electronic box and still achieve large suppression of noise even with long cabling to the sensor head. Rather than using the pick-up coil also for the generation of the compensating field, we decided to add a separate feedback coil (1-layer, 500 turns) on top of the pick-up coil. Thus, we did not create any additional common-mode by asymmetrical loading the pick-up.

Ideally, our feedback range would be $\pm 50 \mu\text{T}$ in order to cover the Earth’s magnetic field. When recalculated with the estimated feedback coil constant (about 108 $\mu\text{A}/\mu\text{T}$) and the supply voltage available ($\pm 2.5\text{V}$), the feedback current sense resistor would be 500 Ω maximum. We also used 1 k Ω and 4.7 k Ω , which however limited the feedback range to $\pm 25 \mu\text{T}$ and $\pm 4 \mu\text{T}$, respectively, in order to show the effect of V/I opamp noise on the feedback noise-field generated in the compensating coil.

Fig. 5a depicts an open-loop measurement, whereas the feedback V/I converter input has been shorted, thus effectively only generating magnetic noise by the feedback coil. We can see that the noise increased with the 500R resistor when compared to the lower range with 4k7. Fig. 5b shows the closed-loop noise, i.e. with the complete

feedback loop running. Also, in this case, the lowest noise is with the lowest range. The peaks are related to the power grid frequency 50 Hz and its 1/3 subharmonic created by the powertrain of a nearby tramway line.

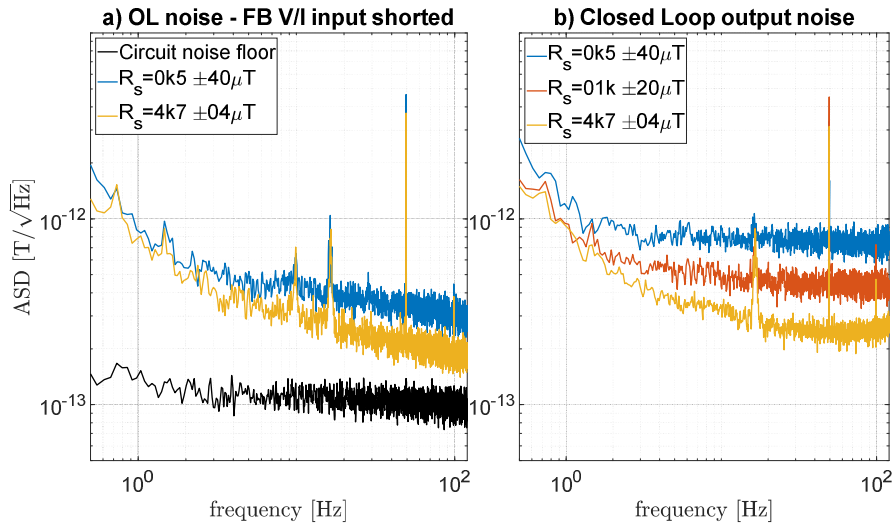


Fig. 5. Trade-off between achievable feedback range and output noise density. a) The effect of feedback V/I converter sense resistor selection on the open loop noise. b) The effect of resistor selection on closed-loop noise parameters.

CONCLUSIONS

We have managed to further lower the white noise of a microwire based magnetometer below 0.3 pT/√Hz @ 8 Hz by optimizing the preamplifier stage and integrating the circuitry and sensor on one PCB board. So far, this is the lowest noise reported for a fluxgate magnetometer. By investigating cross-spectral measurements with multiple sensors / electronic channels, we have verified that the noise of 0.7 pT/√Hz @ 1 Hz is the sensor magnetic noise. Closed-loop operation was also optimized and it finally allowed for sub-pT measurements in compensated feedback loop even for full-field magnetometry.

DATA AVAILABILITY STATEMENT

The data that support the findings of this study are available from the corresponding author upon request.

ACKNOWLEDGMENTS

This work was supported by the Czech Science Foundation, grant no. 20-19686S and CTU Student Grant Competition grant No. SGS20/182/OHK3/3T/13.

1. I. Sasada, *J. Appl. Phys.* **91**, 7789 (2002).
2. R. Bazinet, A. Jacas, G. A. B. Confalonieri, and M. Vazquez, *IEEE Trans. Magn.* **50**, 6500103, (2014).
3. A. Plotkin, E. Paperno, and Alexander Samohin, *J. Appl. Phys.* **99**, 08B305 (2006).
4. M. Butta, and M. Janosek, *AIP Advances* **8**, 047203 (2018).
5. M. Janosek, M. Butta, M. Dressler, E. Saunderson, D. Novotny, and C. Fourie, *IEEE Trans. Inst. Meas* **69**, 2552 (2020).
6. M. Janosek, M. Butta, M. Dressler, E. Saunderson, D. Novotny and C. Fourie, et al., "1 pT-noise fluxgate magnetometer design and its performance in geomagnetic measurements", in 2019 IEEE International Instrumentation and Measurement Technology Conference, edited by IEEE (IEEE, NY, 2019).
7. M. Butta, and B.P. Schutte, *IEEE Trans. Magn.* **55**, 4002906, (2019).
8. M. Butta, S. Yamashita, and I. Sasada, *IEEE Trans. Magn.* **47**, 3748 (2011).
9. S-K. Lee, and M. V. Romalis, *J. Appl. Phys.* **103**, 084904 (2008).
10. F. Han, S. Harada and I. Sasada, *IEEE Trans. Magn.* **50**, 4100305 (2014)

This is the author's submitted version, which in its final form appears in *AIP Advances* **11**, 015347 (2021), <https://doi.org/10.1063/9.0000231>. All rights of the publisher are reserved.